metals

MDPI

Article

Enhancing Aluminum Alloy Properties Through Low Pressure Forging: A Comprehensive Study on Heat Treatments

Silvia Cecchel [1,*] and Giovanna Cornacchia [2]

[1] Streparava SpA, Via Zocco 13, 25030 Adro, BS, Italy
[2] Department of Mechanical and Industrial Engineering, University of Brescia, Via Branze 38, 25123 Brescia, BS, Italy; giovanna.cornacchia@unibs.it
* Correspondence: s.cecchel@streparava.com

Abstract

The weight reduction is a key objective in modern engineering, particularly in the automotive industry, to enhance vehicle performance and reduce the carbon footprint. In this context aluminum alloys are widely used in structural automotive applications, often through forging processes that enhance mechanical properties compared to the results for casting. However, the high cost of forging can limit its economic feasibility. Low pressure forging (LPF) combines the benefits of casting and forging, employing controlled pressure to fill the mold cavity and improve metal purity. This study investigates the effectiveness of the LPF process in optimizing the mechanical properties of AlSi7Mg aluminum alloy by evaluating the influence of three different magnesium content levels. The specimens underwent T6 heat treatment (solubilization treatment followed by artificial aging), with varying aging times and temperatures. Microstructural analysis and tensile tests were conducted to determine the optimal conditions for achieving superior mechanical strength, contributing to the design of lightweight, high-performance components for advanced automotive applications. The most promising properties were achieved with a T6 treatment consisting of solubilization at 540 °C for 6 h followed by aging at 180 °C for 4 h, resulting in mechanical properties of σ_y 280 MPa, σ_m 317 MPa, and A% 3.5%.

Keywords: aluminum alloys; mechanical characterization; automotive; hybrid processes; high-performance

Academic Editors: Huarui Zhang and Lina Jia

Received: 10 June 2025
Revised: 10 July 2025
Accepted: 14 July 2025
Published: 15 July 2025

Citation: Cecchel, S.; Cornacchia, G. Enhancing Aluminum Alloy Properties Through Low Pressure Forging: A Comprehensive Study on Heat Treatments. *Metals* **2025**, *15*, 797. https://doi.org/10.3390/met15070797

1. Introduction

The weight reduction of structural components is a critical aspect to improve fuel or energy efficiency and decrease emissions in the automotive industry, thus aligning production with environmental regulations and enhancing overall vehicle performance. A significant strategy in achieving these goals involves the adoption of aluminum alloys, renowned for their high strength-to-weight ratio [1]. Despite the progress in lightweighting, research is ongoing to balance the reduction of weight with maintaining structural integrity and managing costs, which is especially challenging for heavy vehicles and safety-critical parts. Suspension components, where reliability and safety are paramount, are commonly manufactured through forging processes, which impart superior mechanical properties, including enhanced tensile, yield, and fatigue strength, as well as improved ductility due to better material integrity and chemical uniformity compared to those of castings [2]. Forging processes also refine the microstructure of metals, thereby reducing defects such as voids, porosity, oxide films, inclusions, and coarse intermetallic phases typically found in cast

components [3]. In contrast, casting processes offer a more cost-effective solution suitable for a broader market range, and they are more suitable for producing complex shapes [4]. Recent advancements have focused on enhancing casting processes to mitigate defects. Innovations in low pressure die casting (LPDC), including vacuum riserless/pressure riserless casting (VRC/PRC) and pressure counter pressure casting (PCPC), exemplify significant improvements in casting quality and mechanical properties. VRC/PRC, for instance, allows the molten metal to ascend the casting cavity through specifically pressurized tubes while maintaining a vacuum within the mold cavity [3,5]. Similarly, PCPC involves pressurizing both the casting and furnace chambers simultaneously at approximately equal levels around 0.2 MPa (LPDC typically pressurizes only the furnace chamber between 0.03 and 0.1 MPa). Subsequently, in PCPC, the casting furnace pressure is incrementally raised to a range of 0.23 to 0.3 MPa until solidification is reached, facilitating a controlled ascent of molten metal through the filling tubes and into the casting cavity [6]. These enhancements to the LPDC process have led to higher quality products with a slight increase in mechanical properties. Typical mechanical properties of LPDC (low pressure die casting) components include a yield strength (σ_y) of approximately 210 MPa, an ultimate tensile strength (σ_m) of 280 MPa on average, and an elongation at rupture (A%) of around 5% [3].

Aluminum alloy forgings are characterized by a dense fibrous microstructure achieved through material flow. Mechanical properties depend on the extent and rate of deformation, as well as on temperature conditions, and average values are a yield strength (σ_y) of 290 MPa, an ultimate tensile strength (σ_m) of 330 MPa, and an elongation at rupture (A%) of 8%. However, friction and high shear strains at the interface between the workpiece and the die can induce a recrystallized surface layer, which may compromise component performance [2]. Typically, extruded bars serve as the primary forging stock, while recently, there has been significant interest in an emerging method, the cooling slope (CS) casting process, for producing feedstock for semi-solid processing [7].

In recent years, advancements have focused on hybrid processes that combine the benefits of both casting and forging. Several approaches have been developed to achieve this integration. Initial efforts have explored semisolid processing, which entails forming metallic alloys between their solidus and liquidus temperatures. The microstructure typical of semisolid processed alloys consists of solid spheroids dispersed within a liquid matrix, rather than of dendritic structures [8]. There are presently two primary approaches to semisolid metal forming processes, specifically thixocasting and rheocasting (or stir casting) [3]. Thixocasting involves the creation of a billet through the stirring of the molten metal during bar casting. The billets are subsequently reheated to the semisolid temperature range, followed by their injection into steel dies using die casting machines. This method is capable of producing components of high quality with superior mechanical properties, although at higher manufacturing costs primarily attributable to the specialized feedstock [9,10]. Conversely, rheocasting generates a semisolid slurry from molten metal within a standard die casting furnace adjacent to the machine, which is then transferred to the shot sleeve and injected into the die [9]. Rheocasting effectively mitigates the high cost associated with billet production, making it a more cost-effective alternative to thixocasting. However, its primary drawback lies in the use of single-shot liquid dosing, which can pose challenges in maintaining requisite levels of metal cleanliness. In both processes, excessive injection speed is cautioned against to prevent turbulence and air entrapment [11]. Another category of hybrid processes involves forging a pre-manufactured near-net-shape casting, aimed at maximizing the advantages of both casting (complex shapes at low cost) and forging (enhanced mechanical properties). This approach consists of casting the near-net-shape using traditional methods, followed by removal from the mold. Subsequently, the component undergoes preheating in a furnace, followed by hot forging. Metallurgically,

this process is anticipated to produce components with a more uniform microstructure. The application of hot deformation is expected to further enhance mechanical properties, fatigue resistance, and surface finish [3]. Squeeze casting (SC) is another manufacturing technique in which molten alloy is poured into a preheated die on a hydraulic press. Rapid solidification, which helps eliminate shrinkage porosity, typically occurs under pressures between 50 and 200 MPa [3,12,13]. Metal injection speeds are reduced to about 0.5 m/s to minimize turbulence, compared to the 30 to 60 m/s used in high-pressure die casting (HPDC) [10]. SC components offer advantages such as superior mechanical properties, refined structure, and minimal porosity. However, challenges include high capital costs, reduced die longevity, and constraints on maximum size and weight. [12].

Ultimately, the integration of the advantages provided by the aforementioned hybrid processes, along with a reduction in their associated drawbacks, has led to the development of a novel technique known as low pressure forging (LPF). In the LPF process, the molten metal fills the die cavity under pressure from an inert gas, similar to the principles employed in low pressure die casting (LPDC). This approach ensures a cleaner melt and reduces porosity compared to the results for techniques such as squeeze casting (SC). After the cavity is filled, a "closing shutter" piston (Figure 1) blocks the flow of molten metal, followed by the application of pressure using a secondary "forging piston" concentric to the position of the former (also shown in Figure 1). Notably, the pressure application occurs within the casting machine itself, eliminating the need for separate heating stages and presses at secondary stations. LPF pressure values typically range between 90 and 270 MPa [14]. The abovementioned features allow LPF to take advantage of both casting and forging processes in a smarter way, while enhancing melt purity through its filling method. This study will concentrate specifically on evaluating the efficacy of LPF in achieving superior mechanical properties and reduced defects in aluminum alloys.

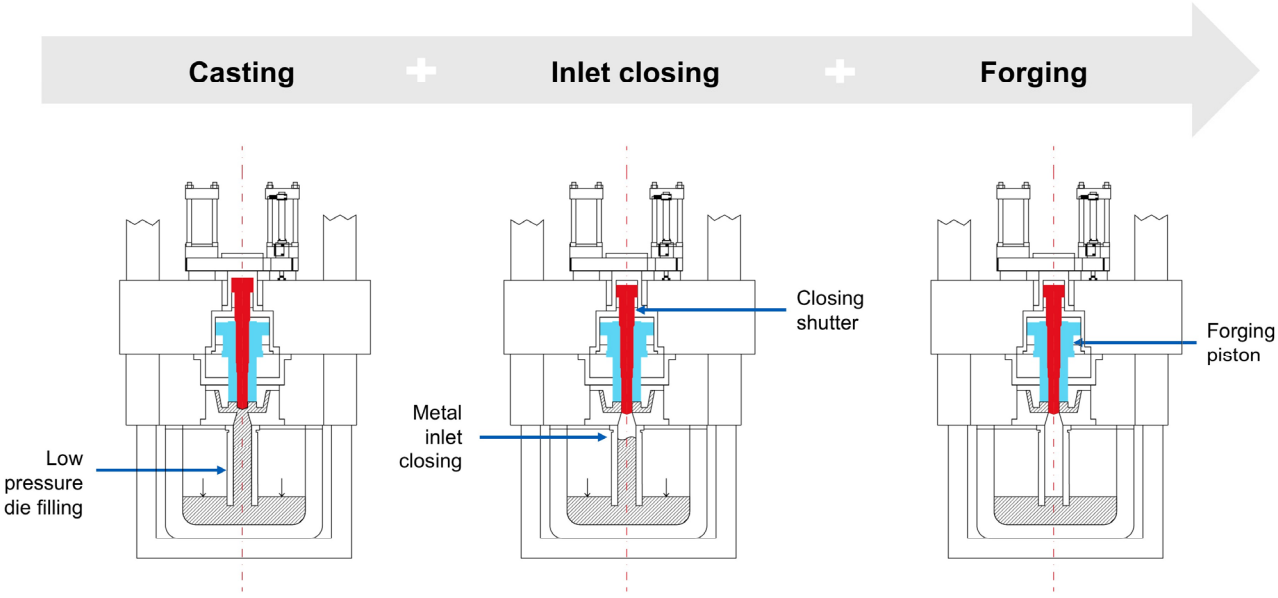

Figure 1. Low pressure forging process scheme.

Chemical composition significantly influences the mechanical properties of aluminum alloys used in these applications. One of the most widely used aluminum alloys for these applications is A356 (AlSi7Mg0.3). The aging behavior of Al–Mg–Si alloys is primarily related to the formation of the β-Mg_2Si phase. Higher magnesium content (% Mg) typically leads to an increased volume fraction of β precipitates, thereby enhancing strength [15,16]. Optimal strengthening effects are observed up to approximately 0.4% Mg, beyond which

the presence of the π-phase ($FeMg_3Si_6Al_8$) stabilizes, limiting the availability of Mg for strengthening β-Mg_2Si precipitates. The standard composition of A356 alloy spans a wide range of Mg content (0.25–0.45%), whereas A357 includes higher Mg levels (0.4–0.7%) and elevated beryllium percentages (0.04–0.07%), not permissible in A356 [15]. The influence of Mg content on the mechanical properties of Al–Si casting alloys has been widely investigated. G.K. Sigworth et al. [17] found that raising Mg levels from 0.06% to 0.44% leads to improvements in tensile properties, and the reduction in ductility is more than offset by the strength gains. Moreover, the research of C.H. Ca'ceres [18] observed that maintaining the Mg content below 0.5% is key to avoiding the precipitation of the $Al_8Mg_3FeSi_6$ phase, thus optimizing the properties of 356/357 alloys under various conditions.

These variations necessitate deeper exploration, particularly concerning their impact on emerging semisolid processes like LPF. Similarly, T6 heat treatments for Al–Si–Mg alloys require thorough investigation to optimize the mechanical properties relative to specific alloys and processing techniques. The ultimate goal is to establish a tailored framework of processes, materials, and heat treatments capable of achieving mechanical benchmarks that are challenging to attain using conventional casting methods.

The present study investigates the effects of the innovative low pressure forging (LPF) process on the mechanical properties of AlSi7Mg aluminum alloy using three different magnesium content levels. Specimens produced under these conditions underwent T6 heat treatment with varying aging times and temperatures to determine the optimal parameters for the intended application. Microstructural analysis and tensile tests were conducted to evaluate the results. The challenging threshold selected for this research includes a yield strength (σ_y) of 250 MPa, an ultimate tensile strength (σ_m) of 310 MPa, and an elongation at rupture (A%) of 5%, thus providing significant improvement in mechanical strength compared to that of traditional LPDC.

2. Materials and Methods

2.1. Sample Description

Approximately 150 tensile specimens were cast using a specifically designed mold capable of producing three samples per casting, as illustrated in Figure 2. The low pressure forging (LPF) device at the Alunext srl plant (Sirone (LC), Italy) was utilized for production. The raw alloy was melted at 750 °C and poured in low pressure die casting (LPDC) mode, with a pressure of approximately 0.35 bar, into a mold pre-heated to 350 °C. Subsequently, the closing shutter was activated to block the metal filling, and a pressure of about 72 MPa was applied by the forging piston in the central section of the mold (indicated by the red arrow in Figure 2).

Three samplings batches were prepared using aluminum A356 alloy with varying magnesium content, as detailed in Table 1, to assess its impact on the mechanical properties. Chemical composition was calculated by means of optical emission spectroscopy, following the ASTM E1251-24 standard [19].

The components underwent T6 heat treatment under various conditions to evaluate the resulting mechanical properties. The target application for this process is the production of automotive structural components with the following mechanical properties: a yield strength (σ_y) of 250 MPa, an ultimate tensile strength (σ_m) of 310 MPa, and an elongation at rupture (A%) of 5%. The process setup, materials, and heat treatment were designed to achieve these targets. Consequently, the heat treatment parameters were selected based on an extensive literature review to meet the desired mechanical properties. Table 2 summarizes the tested conditions in terms of chemical composition and heat treatment parameters. T6 heat treatments were performed with a solution treatment at 540 °C for 6 h, followed by water quenching. This value is recommended in most references for

semisolid [15] and traditional [20–22] casting methods and is widely used in the production of this alloy. It is important to note that the variation in mechanical properties is primarily influenced by aging time and temperature [20,21]. Thus, the aging times and temperatures for each chemical condition tested varied, as shown in Table 2. It can be observed that the experimental analyses were accomplished across a wider range of thermal treatment parameters for the conditions with low and high magnesium content. Based on the results of this initial experimental campaign, three heat treatment conditions that exhibited the highest potential for achieving the target mechanical properties were identified. The Mg medium composition was subsequently studied to introduce an intermediate assessment point between the two extreme compositions. Therefore, the Mg medium was tested under the three pre-selected optimal heat treatments parameters derived from the experimental outcomes obtained for the Mg low and Mg high conditions (see Table 2). A comparison with the as-cast condition was also conducted for all compositions.

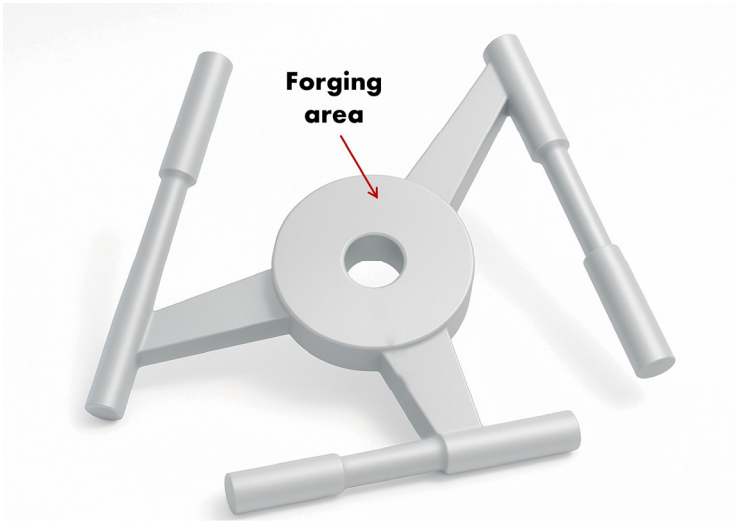

Figure 2. Scheme of the sample die. The red arrow indicates the area where pressure is applied by the forging piston.

Table 1. Chemical composition of the LPF samples.

Alloy (wt.%)	Al	Si	Fe	Cu	Mn	Mg	Ti
Mg low	Bal.	7.22	0.20	0.005	0.006	0.24	0.09
Mg medium	Bal.	7.10	0.22	0.005	0.006	0.35	0.10
Mg high	Bal.	7.37	0.21	0.006	0.006	0.49	0.10

Table 2. Summary of chemical composition and heat treatment parameters of the samples. Solubilization is fixed ad 540 °C for 6 h.

Aging Parameters		Tested Condition per Alloy	
T (°C)	t (h)	Mg Low and Mg High	Mg Medium
160	8	x	
	10	x	
180	4	x	x
	6	x	
	8	x	x
200	2	x	
	4	x	x

2.2. Metallographical Analysis

For metallographic observations, samples from different conditions were sectioned orthogonally from the shoulders of the tensile specimens to ensure a representative microstructure. The samples were prepared using standard metallographic techniques. Initially, the samples were ground using silicon carbide (SiC) paper up to 4000 grit to achieve a smooth surface. This was followed by polishing with 1 µm diamond paste to obtain a mirror-like finish, which is crucial for high-quality microscopic examination. To reveal the microstructure, the polished samples were examined using a Leica DMI 5000 M optical microscope (OM) (Leica Microsystem, Milan, Italy). The highlighted microstructure was also observed using a LEO EVO 40 scanning electron microscope (SEM) (Zeiss, Milan, Italy) operated at a 20 kV acceleration voltage with a working distance of 11 mm. Semi-quantitative chemical analyses were obtained by means of an EDS (energy dispersive spectroscopy–link analytical eXL) probe, with an acquisition time of 120 s per spectrum to ensure adequate counting statistics for reliable compositional analysis. Data acquisition and processing were performed using Oxford Instruments INCA 4.11 software. The samples were prepared by standard metallographic polishing and coated with gold to prevent charging effects in order to evaluate the nature of the precipitates. This metallographic analysis provided valuable insights into the relationship between the microstructure and the mechanical properties of the alloy under different heat treatment conditions.

2.3. Hardness and Tensile Tests

Vickers microhardness test profiles were carried out along the diameter of each traverse surface of the tensile specimens shoulders. Preliminary analyses were conducted to assess the representativeness of the microstructure in the heads of the specimens, which led to the selection of this area as representative of the overall microstructural features. According to ASTM E92-23, a Mitutoyo HM-200 instrument was used [23], applying 300 gf load for 15 s.

For the tensile tests, cylindrical samples with the geometry shown in Figure 3 were used. The samples were tested in their unmachined state to evaluate conditions comparable to those of the actual component surface. The tensile tests were conducted using an electromechanical testing machine, Instron 3369 (Instron, Norwood, MA, USA), equipped with a 50 kN load cell. The tests were carried out at a strain rate of 2 mm/min at room temperature, in accordance with UNI EN ISO 6892–1:2020 [24]. Key mechanical properties, including yield strength (σ_y), ultimate tensile strength (σ_m), and elongation after fracture (A%), were calculated. Strain measurements were obtained using a 50 mm extensometer to ensure precise deformation readings.

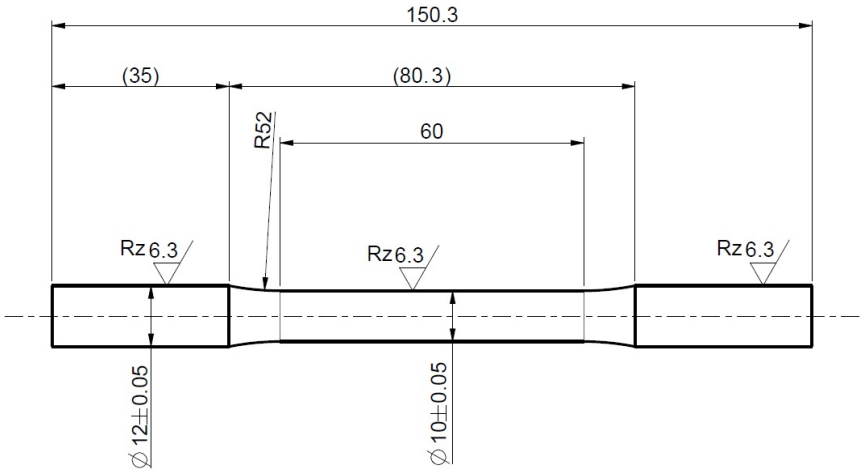

Figure 3. Tensile test specimen geometry, with dimensions in mm.

3. Results and Discussion

Given the targeted mechanical properties presented in the introduction, the effect of the LPF process is an effective refining of the as-cast microstructure, composed in general of small α-aluminum dendrites and interdendritic Al–Si eutectic regions with iron-rich intermetallics. Then, the T6 treatment (solution treatment, quenching, and aging) was carefully tailored to achieve an optimal microstructural homogenization and precipitation hardening that meet the desired strength and ductility criteria.

The following general considerations are provided to contribute to a more thorough contextualization and elucidation of the analyses undertaken in this work. In Al–Si–Mg alloys, the optimal balance between strength and ductility achieved after the thermal treatments is ascribed to the modification of Si particle characteristics during the solution treatment and to the formation of non-equilibrium β (Mg_2Si) precipitates during the aging process [25]. Indeed, the eutectic regions in the as-cast state are usually defined by acicular particles, which can be coarse and interconnected, with shapes acting as crack initiation sites and adversely affecting mechanical performances. Following a solution treatment at 540 °C for 6 h, rapid quenching not only suppresses coarse precipitate growth but also preserves a supersaturated solid solution. In this quenched state, the overall microstructure becomes more homogeneous with dissolution of the Mg_2Si particles. The eutectic silicon phase experiences significant morphological changes; solubilization drives its transformation from a sharp, acicular form to a more rounded, globular shape. This modification is crucial from a mechanical standpoint since a globular silicon morphology minimizes stress concentration at the silicon–matrix interface, thereby enhancing ductility and fatigue resistance. Furthermore, the synergistic effect of LPF-induced dendrite fragmentation and quenching-induced spheroidization establishes an optimal microstructural foundation, facilitating a uniform precipitation process during subsequent aging treatments. The resulting microstructure is more uniform and provides an optimized baseline for subsequent thermal treatments, especially when combined with quenching. In particular, the aging process is primarily governed by the precipitation of strengthening phases, especially the β-Mg_2Si phase, whose optimal volume fraction is typically achieved at a specific Mg content [15,16]. Furthermore, the microstructure also develops precipitates such as isolated silicon particles and acicular FeMgSiAl compounds. In particular, the FeMgSiAl compounds tend to stabilize, thereby limiting the availability of Mg for the formation of β-Mg_2Si precipitates. According to literature, the optimal strengthening effects are observed up to approximately 0.4% Mg.

3.1. Metallographical Analysis

Figure 4 reports representative microstructures of the A356 alloy produced by conventional LPDC (left) and LPF (right) under identical magnification and imaging conditions for direct comparison. It is clear from these images that the application of LPF effectively reduces the dendritic network in comparison to that of the traditional LPDC method.

The investigation began by examining the extremes of Mg content, i.e., low and high Mg alloys (see Figures 5 and 6, respectively), before extending the study to medium Mg alloys (see Figure 7), based on insights derived from the overall investigations (comprising tensile and hardness tests) of the former Mg contents. In both low and high Mg alloys processed through low pressure forging (LPF), the as-cast condition exhibits a partially refined microstructure compared to that of conventional casting methods. High-resolution micrographs reveal that the LPF process modifies the conventional dendritic network, promoting a transition of the aluminum-rich primary phase toward a more globular or semi-globular structure, while the eutectic silicon phase largely retains its acicular morphology in the as-cast state, as expected. In both Figures 5 and 6, the effect of solubilization is clear in the as-quenched state micrographs: the eutectic silicon presented a globular shape,

and the intermetallic particles are rounded. Green, yellow and red arrows indicated Al–Si intermetallic, π-AlFeMgSi, and β-AlFeSi alloys, respectively.

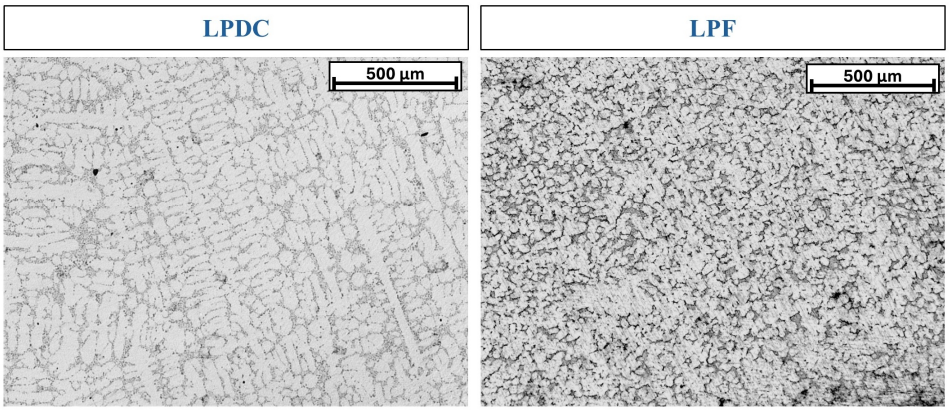

Figure 4. Representative microstructures of the A356 alloy produced by LPDC (**left**) and LPF (**right**).

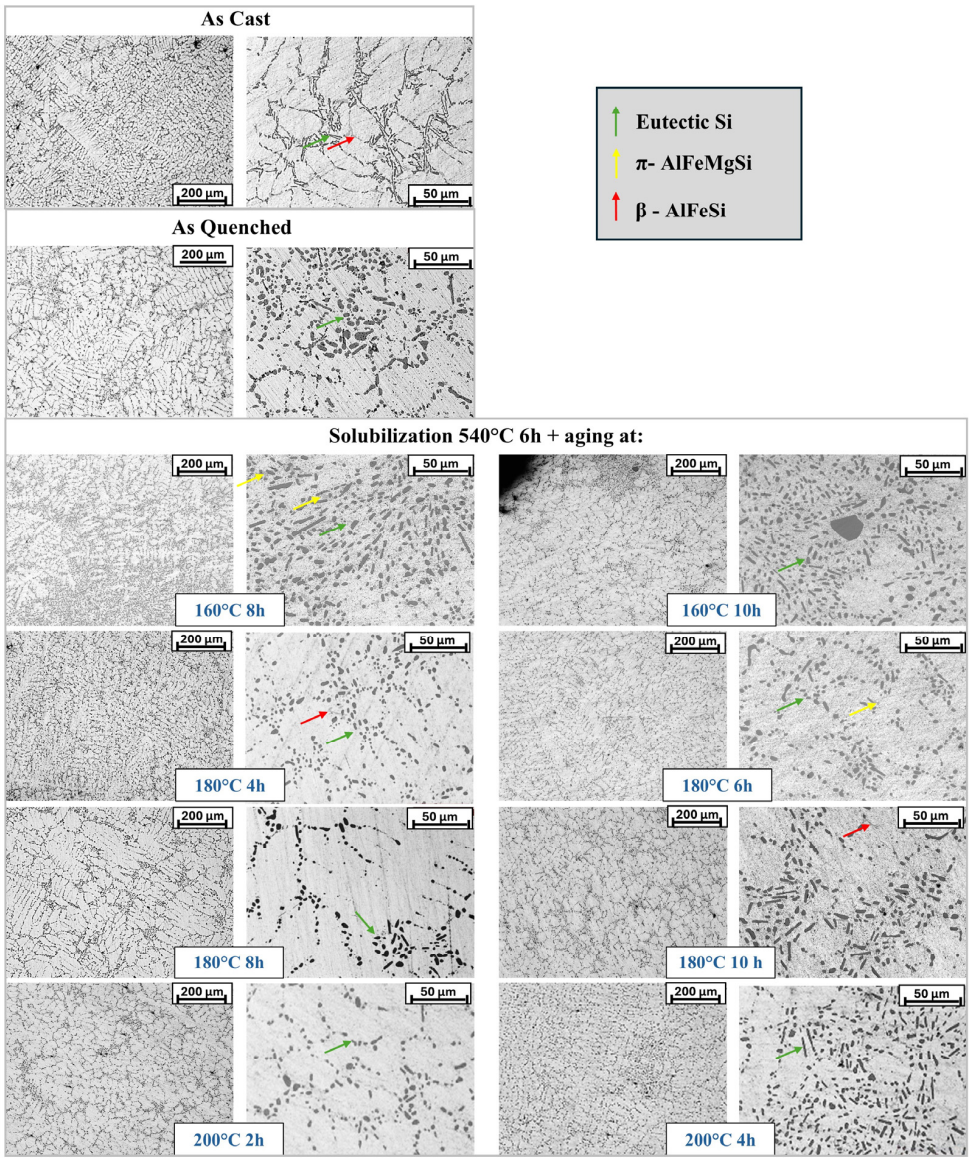

Figure 5. Microstructures of A356 alloy with low magnesium content, observed at different aging treatment conditions and magnifications.

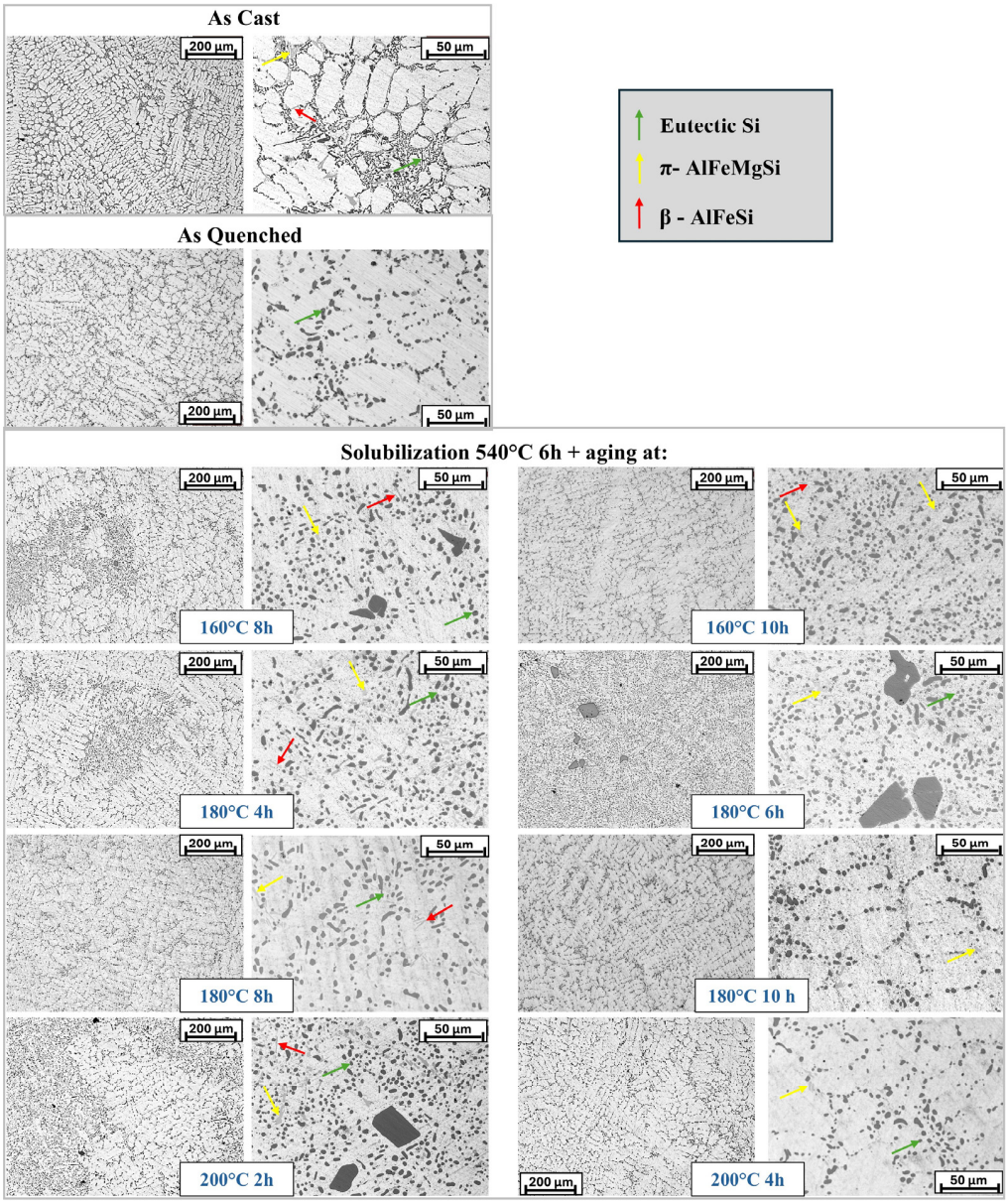

Figure 6. Microstructures of A356 alloy with high magnesium content, observed at different aging treatment conditions and magnifications.

Aging treatments at 160 °C, 180 °C, and 200 °C induce significant microstructural evolution with distinct kinetic behaviors. At 160 °C, the precipitation kinetics were relatively slow. In low Mg alloys aged for 8 h, fine precipitates begin to form uniformly, although their density remains lower than that achieved at higher aging temperatures. Even when the aging period is extended to 10 h, the morphological changes are modest, reflecting a diffusion-limited process. Similar trends are observed in high Mg alloys, where fine precipitates develop along the refined interdendritic regions, with only minor modifications upon prolonged aging. From an optical microstructural point of view, no remarkable effect is observed with varying the aging time. The comparison between Figures 5 and 6 confirms that increasing the magnesium content generally results in an increased presence of AlFeMgSi precipitates (light grey, yellow arrows). The other characteristics remain unchanged.

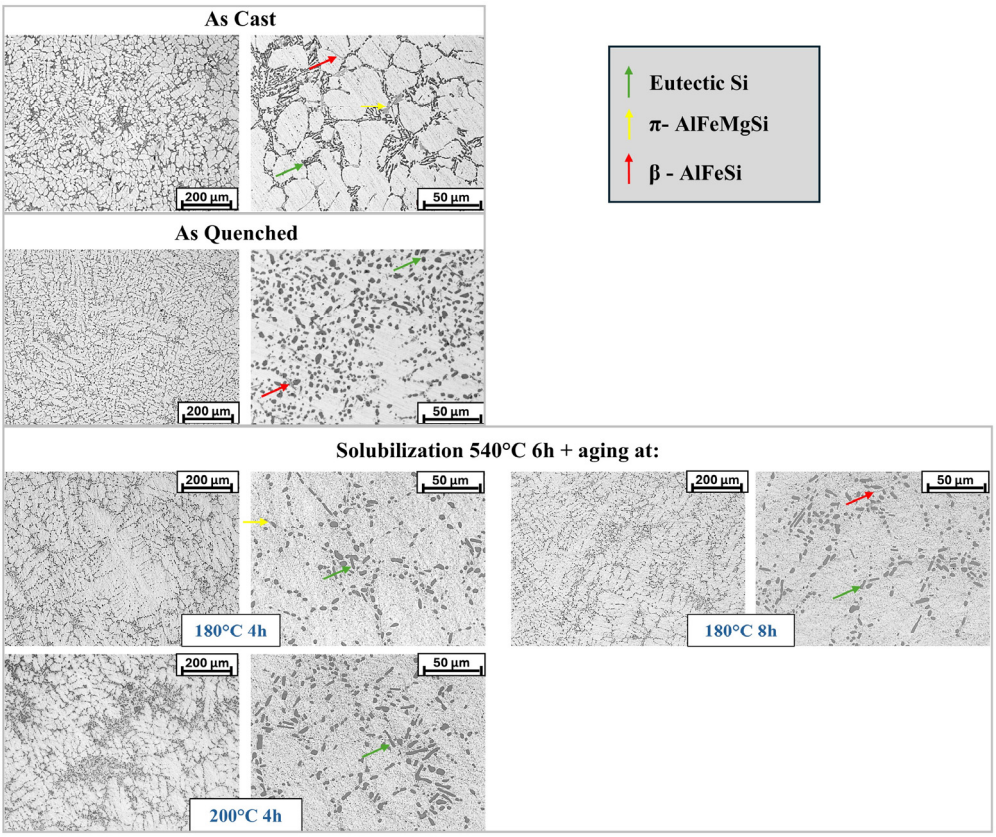

Figure 7. Microstructures of A356 alloy with medium magnesium content at different magnifications and under different aging conditions.

When subjected to aging treatments at 160 °C, 180 °C, and 200 °C, medium Mg alloys respond in a manner similar to that of the extreme cases (see Figure 7).

In order to gain a deeper understanding of the nature of the intermetallic phases, Figure 8 reports SEM observations and EDS semi-quantitative chemical analyses of LPF samples under both low and high Mg conditions. The analysis confirmed that the microstructure is composed of intermetallic phases, identifiable as β-AlFeSi phase (red arrow) and π-AlFeMgSi Chinese script phase (yellow arrow). It is worth noting that although π-AlFeMgSi is an Fe-rich intermetallic phase that may cause embrittlement of the alloy, the transformation of the needle-like β-AlFeSi phase into the Chinese script π-AlFeMgSi phase mitigates the detrimental effects of the former on mechanical properties. This transformation mechanism is known to occur with increasing Mg content in the presence of Fe [26]. Overall, a higher amount of π-AlFeMgSi was observed in the high Mg alloy, as also confirmed by optical microscopy investigations. Moreover, the β-AlFeSi particles underwent significant fragmentation, resulting in a reduced average size, as indicated by the white arrows.

In conclusion, the following considerations emerge as consistently applicable across the range of magnesium content conditions investigated. The application of LPF effectively reduces the dendritic network in the as-cast condition, transforming it into a more semi-globular structure. This refinement is further enhanced by solubilization and quenching, which promote the fragmentation and spheroidization of Al–Si eutectic structures and its homogenization in the α-aluminum matrix and establishes a supersaturated solid solution. Moreover, the intermetallic phases appear rounder and smaller compared to those observed in the as-cast condition; this feature is already evident in the as-quenched state and is retained with comparable morphology after aging.

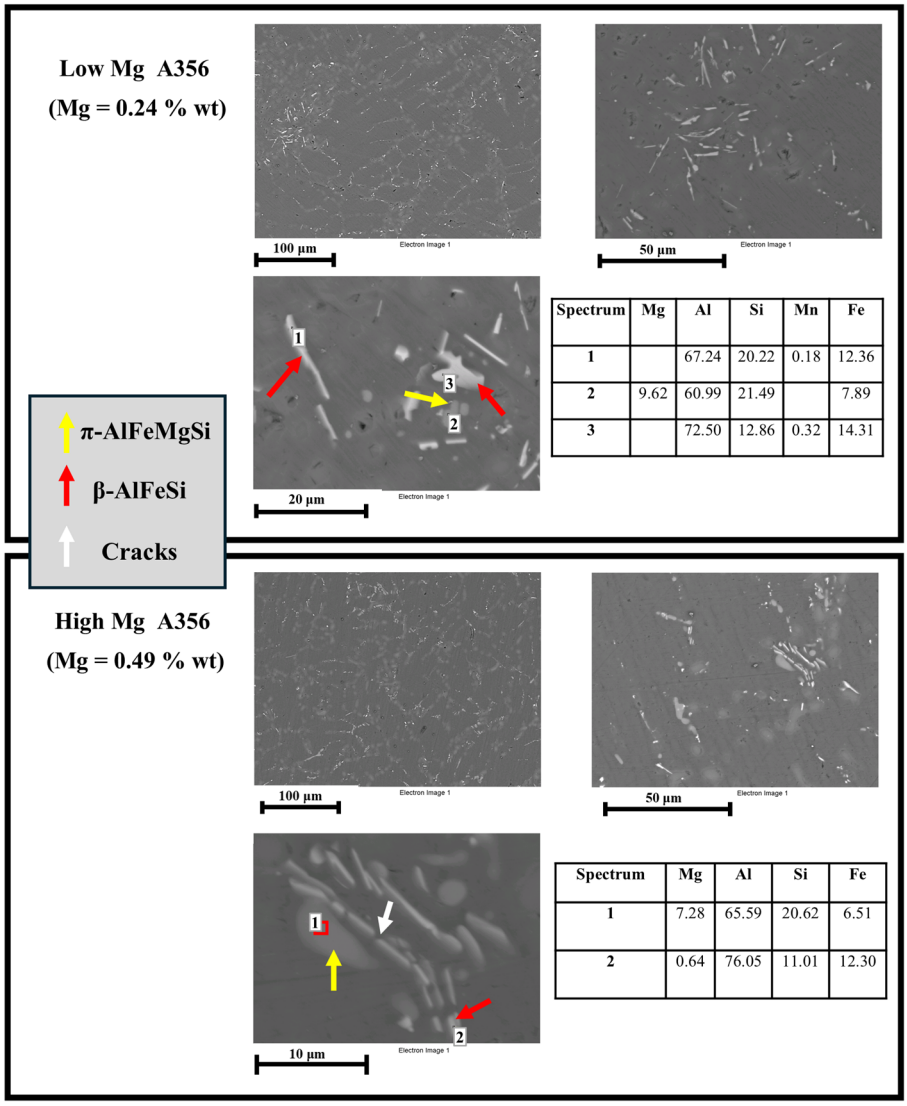

Figure 8. SEM images and EDS analysis of EN AC 42100-T6 low Mg and high Mg samples produced using LPF. All elements are expressed in wt%.

3.2. Hardness and Tensile Tests

Figure 9 displays the tensile curves for the analyzed conditions. Table 3 reports the tensile properties of the complete set of heat treatment parameters and chemical compositions analyzed (Mg high, Mg medium, and Mg low). In these initial experimental campaigns of the challenging process under investigation, some defects (i.e., eutectic segregation, porosity, inclusions) were observed. Consequently, during this stage, it was not possible to guarantee an extensive statistical analysis associated with the numerous processing and post-processing variables currently under investigation. Thus, the mechanical properties were analyzed based on the best-performing specimen in terms of yield strength, a criterion considered to best represent the potential of the process. Future developments will aim to reduce this variability, with the goal of improving reproducibility. It is worth noting that yield strength is the most relevant property for this category of structural automotive components, which are typically designed based on this specific mechanical characteristic. For such applications, the material must exhibit a sufficient level of ductility, although generally, a high elongation percentage is not required.

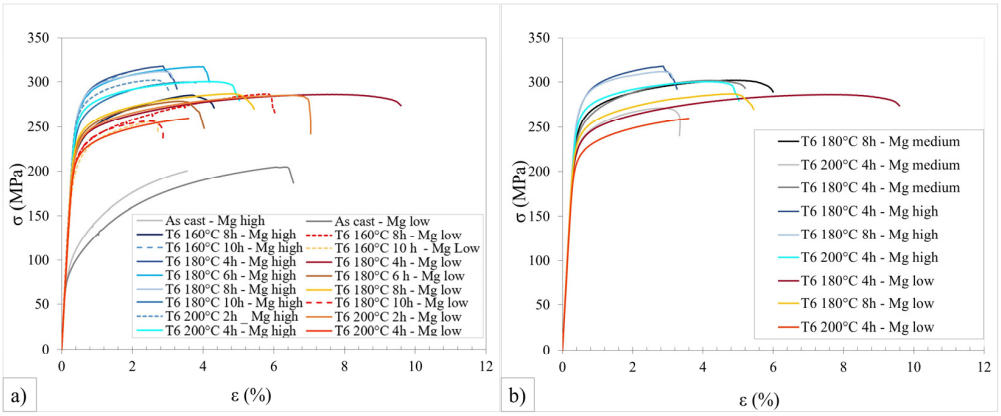

Figure 9. Tensile curves showing (**a**) the complete set of heat treatment parameters and the first chemical compositions analyzed (Mg high and Mg low) and (**b**) the optimal heat treatment parameters selected for each chemical composition under investigation (Mg high, Mg low, Mg medium).

Table 3. Tensile properties of the complete set of heat treatments and the chemical compositions analyzed.

			σ_y [MPa]	σ_m [MPa]	A [%]
F	As-cast	Mg high	106	200	3.0
		Mg low	96	205	6.0
T6 540 °C 6 h +	160 °C 8 h	Mg high	230	286	3.9
		Mg low	217	287	5.7
	160 °C 10 h	Mg high	276	310	1.5
		Mg low	211	257	2.4
	180 °C 4 h	Mg high	280	317	3.5
		Mg medium	249	302	4.8
		Mg low	236	278	7.2
	180 °C 6 h	Mg high	277	317	3.8
		Mg low	251	272	3.7
	180 °C 8 h	Mg high	279	311	3.0
		Mg medium	255	302	5.6
		Mg low	242	287	5.0
	180 °C 10 h	Mg high	257	300	4.0
		Mg low	222	257	3.0
	200 °C 2 h	Mg high	270	302	3.0
		Mg low	232	285	7.0
	200 °C 4 h	Mg high	265	300	5.0
		Mg medium	235	272	3.0
		Mg low	219	260	3.0

Specifically, Figure 9a presents all the investigated heat treatment parameters, including the as-cast baseline, for the chemical compositions defined as Mg low and Mg high. It should be noted that blue color shades are used for the curves representing the Mg high condition, whereas yellow to red shades are used for the Mg low condition. From these data, it is evident that samples with a higher Mg content achieve increased yield and ultimate tensile strengths, although with reduced elongation percentages compared to those of their low Mg counterparts.

Considering the challenging mechanical properties desired from the process (σ_y 250 MPa, σ_m 310 MPa, A% 5%), the heat treatments at 160 °C fail to meet these

requirements; indeed, only the 10 h aging at 160 °C in the high Mg alloy approaches these target strengths, but it exhibits low ductility (σ_y 276 MPa, σ_m 310 MPa, A% 1.5%). Consequently, all of the 160 °C conditions are disregarded with respect to the full set of mechanical property criteria.

Overall, the most favorable results occur at 180 °C, even at an aging time of 4 h. The stress–strain curves at 180 °C for 4 and 8 h are comparable, while characteristics of overaging emerge at 10 h. These trends hold for both chemical compositions, with the low Mg alloy especially demonstrating lower mechanical strengths with higher elongation. The 200 °C aging treatment yields moderately promising outcomes only for the 4 h aging time in the high Mg alloy, meeting the yield strength and ductility targets but falling slightly short regarding ultimate tensile strength. Nevertheless, the overall mechanical performance is inferior to that achieved with treatments at 180 °C.

Accordingly, a subset of heat treatment parameters was selected for further mechanical and microstructural evaluation on intermediate Mg samples: 180 °C for 4 h and 8 h, and 200 °C for 4 h. Figure 9b presents the tensile curves for these selected heat treatments across all the chemical compositions examined, namely high, low, and medium Mg.

As expected, the Mg medium alloy exhibits intermediate mechanical properties. For all chemical compositions examined the 180 °C for 4 h, this treatment provides the highest performance; extending the aging time to 8 h yields no significant improvement, as can be seen from data reported in Table 3. Please note that the configuration selected as the most promising falls slightly short, solely in terms of elongation (3.5% vs. 5%), of the mechanical property threshold identified by the authors for the intended application due to the defects observed during these campaigns. It is worth noting, however, that the yield strength significantly exceeds the proposed threshold and given that this is one of the primary design-relevant properties, the potential of the process appears very promising. Future process developments will aim to reduce defect-related issues, thereby improving reproducibility and achieving higher elongation values, even in the configurations showing the highest yield strength.

These observations are also represented in Figure 10, where yield and ultimate tensile strengths are plotted for each condition, alongside the performance ranges for standard LPDC and forging processes and the LPF process challenging the mechanical threshold properties of those desired from the process. Based on this analysis, the optimized heat treatment cycle is designated as T6, consisting of solutionizing at 540 °C for 6 h, quenching, and aging at 180 °C for 4 h. The high Mg alloy achieves mechanical properties well above to the design targets in terms of yield strength and ultimate tensile strength, although with reduced elongation; further process refinement is expected to enhance ductility. Overall, the values are promising, thanks to this initial development of an innovative process combined with the most appropriate heat treatment parameters and alloy compositions. Indeed, it can be noted that the achieved properties are well above those typically associated with standard LPDC and closely approach those of the forged components.

Figure 11 reports the HV microhardness profiles across the transverse section from the shoulders of the tensile specimens for each condition. In particular, the as-cast profiles and the full set of analyzed heat treatment parameters are reported in Figures 11a and 11b for the chemical compositions Mg high and Mg low, respectively, while Figure 11c shows the selected optimal heat treatment parameters for all examined chemical compositions (Mg high, Mg low, Mg medium). Table 4 summarizes the average HV microhardness values and corresponding standard deviations for all analyzed conditions.

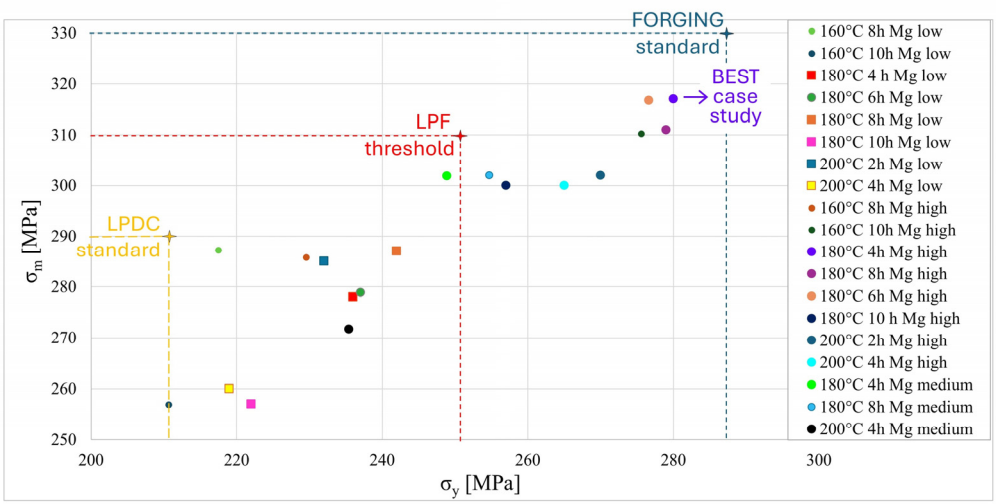

Figure 10. Ultimate tensile strength as a function of yield strength for all conditions tested under tensile loading. The plot also includes the typical property ranges for LPDC and forging technologies, as well as the target values for the LPF process.

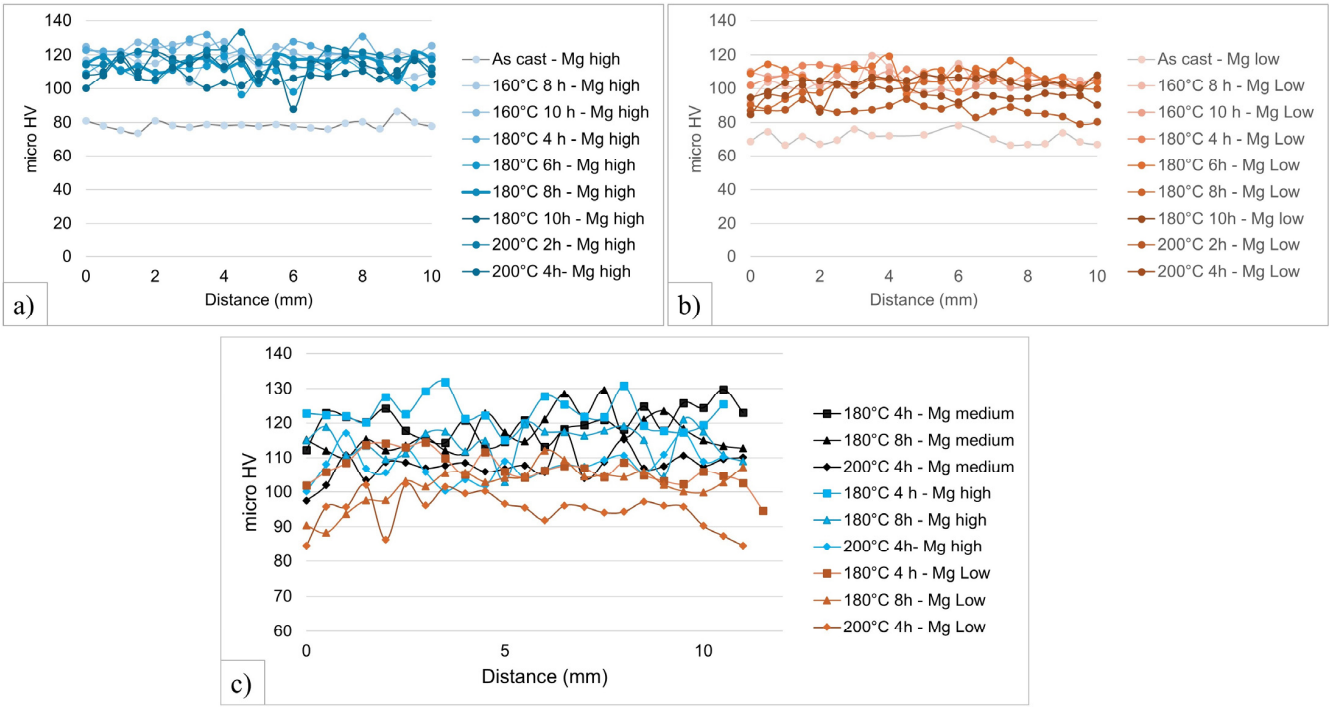

Figure 11. HV microhardness plots for the full set of analyzed heat treatment parameters for the chemical compositions (**a**) Mg high and (**b**) Mg low, and (**c**) the selected optimal heat treatment parameters for all examined chemical compositions (Mg high, Mg low, Mg medium).

The as-cast Mg low alloy exhibits a lower average hardness (70 HV) compared to that of the Mg high (78 HV). The microhardness profiles also show lower values for the Mg low condition after the various heat treatments, with average values ranging from 86 to 111 HV, compared to the Mg high condition, which exhibits average values between 108 and 123 HV. It is evident that increasing the magnesium content yields a slightly more pronounced response to heat treatment, with the Mg high condition showing an average hardness improvement over the as-cast state of approximately 40 HV, compared to about 30 HV for the Mg low condition. The 200 °C treatments generally result in lower hardness values compared to the results for the other temperature parameters across all the chemical

compositions examined. Among the 160 °C treatments, the 10 h treatment for the Mg high composition is particularly noteworthy, with one of the highest average values recorded (123 HV). For completeness, it should be mentioned that this condition exhibits a low percentage of elongation in the tensile tests, a factor not evident in the present hardness characterization. Regarding 180 °C, it appears that is results in overaging starting from the 8 h condition. In fact, the 8 and 10 h times show a decrease in hardness of about 10 HV points for both the Mg low and the Mg high condition, compared to the results for the shorter treatment times.

Table 4. Average HV microhardness values and corresponding standard deviations for all analyzed conditions.

		Mg Low		Mg High		Mg Medium	
Aging Temperature (°C)	**Aging Time (h)**	**Avg. HV**	±	**Avg. HV**	±	**Avg. HV**	±
160	8	111	6	114	5		
	10	104	4	122	3		
180	4	107	5	123	4	120	5
	6	114	6	122	4		
	8	102	6	114	5	117	5
	10	104	3	113	7		
200	2	86	5	118	5		
	4	95	5	108	4	108	4

For the chosen aging conditions, Mg medium exhibits hardness levels comparable to those of Mg high and exceeding those of Mg low. A slight performance decrease is noted for the 180 °C for 8 h condition compared to the 180 °C for 4 h condition, indicating a potential onset of overaging. The maximum hardness is achieved in Mg high following aging at 180 °C for 4 h. This finding is validated both from the analysis of the graph in Figure 11c and from the data reported in Table 4.

4. Conclusions

The increasing demand for aluminum alloys for use in automotive structural components, driven by lightweighting needs requirements, necessitates advanced manufacturing processes that can deliver superior mechanical properties. The present study investigated the effects of the innovative low pressure forging (LPF) process on enhancing the mechanical properties of AlSi7Mg aluminum alloy. Three different magnesium content levels (0.24%, 0.35%, and 0.49%) were examined under T6 heat treatment conditions, with fixed solubilization parameters (540 °C for 6 h followed by quenching) and varying aging times and temperatures. Comprehensive microstructural analysis, hardness measurements, and tensile tests led to the following conclusions.

The microstructural investigation revealed the following:

- The LPF process effectively refines the as-cast microstructure, transforming conventional dendritic networks into more semi-globular structures and reducing porosity compared to the results for traditional casting methods.
- Solution treatment and quenching further enhance this refinement by promoting the fragmentation and spheroidization of Al–Si eutectic structures, transforming silicon particles from an acicular form to a more rounded, globular shape that minimizes stress concentration. Intermetallic phases appear rounder and smaller compared to those of the as-cast condition, with this feature being evident in the as-quenched state and retained with comparable morphology after aging.

- With increasing magnesium content, there is a greater presence of π-AlFeMgSi Chinese script intermetallics, representing a beneficial transformation from the more detrimental needle-like β-AlFeSi phases.
- SEM–EDS analysis confirmed the conversion of needle-like β-AlFeSi phases into the Chinese script π-AlFeMgSi morphology.

The hardness and tensile tests revealed the following:

- Mg content impact: higher Mg levels result in improved hardness, yield, and ultimate tensile strengths, accompanied by a slight reduction in elongation compared to that noted for the low Mg conditions.
- For treatments at 160 °C, only the 10 h aging for Mg high nearly meets the strength targets (σ_y 276 MPa, σ_m 310 MPa), yet with insufficient elongation (A% 1%); other conditions are at inadequate this temperature for the desired mechanical properties.
- Treatments at 200 °C provide generally lower mechanical properties than those obtained from the 180 °C treatments, with only partially acceptable results for Mg high at 4 h (σ_y 265 MPa, σ_m 300 MPa, A% 5%).
- Treatments at 180 °C yield the best overall performance, with a time of 4 h proving optimal. The results at 8 h are very similar to those at 4 h, and since the performance is comparable, a shorter treatment duration is preferable. Signs of overaging begin to appear at 10 h, as evidenced by a decrease in hardness values by approximately 10 HV for both low and high Mg conditions.
- The optimal process is a T6 cycle (solution at 540 °C for 6 h, water quenching, and aging at 180 °C for 4 h) with high Mg content (0.49%), which best meets the strength targets, despite slightly reduced elongation (σ_y 280 MPa, σ_m 317 MPa, A% 3%).
- Medium Mg content (0.35%) represents a promising compromise, achieving nearly all target mechanical properties (σ_y 249 MPa, σ_m 302 MPa, A% 5%), while balancing strength with acceptable ductility.

In conclusion, these results demonstrate a significant improvement in mechanical performance using the LPF process compared to the results for traditional LPDC. The property enhancements are already evident in the standard A356 alloy, namely low and medium magnesium conditions, while a targeted increase in magnesium content can be beneficial for applications requiring higher yield strength. Even for conventional compositions, the LPF process demonstrates its potential by maximizing mechanical properties beyond what is typically achievable with standard casting methods. The optimized heat treatment parameters ensure the achievement of good performance levels that approach those of conventional forging, while maintaining the benefits of the casting processes. Future developments will focus on process and tooling improvements, working with full-scale components to better assess the repeatability of properties and to optimize the performance balance between strength and ductility. Additional aspects to be investigated in the next steps of the research include the applicability of recycled alloys, even in the current class of components where the structural requirements are particularly stringent.

Author Contributions: Conceptualization, S.C.; methodology, S.C.; validation, S.C. and G.C.; formal analysis, S.C. and G.C.; investigation, S.C. and G.C.; resources, S.C. and G.C.; data curation, S.C. and G.C.; writing—original draft preparation, S.C.; writing—review and editing, S.C. and G.C.; visualization, S.C.; supervision, S.C. and G.C.; project administration, S.C. and G.C.; funding acquisition, S.C. and G.C. All authors have read and agreed to the published version of the manuscript.

Funding: This research received no external funding.

Data Availability Statement: The data presented in this study are available on request from the corresponding author due to commercial reasons.

Acknowledgments: The authors are grateful to Aurelio Ricciardi from Alunext for providing support during production and to Claudio Gislon from Co.stamp for contributions to the tooling development.

Conflicts of Interest: Author Silvia Cecchel is affiliated with Streparava SpA. This affiliation did not influence the scientific outcomes of the work. The authors declare that the research was conducted in the absence of any commercial or financial relationships that could be construed as a potential conflict of interest.

References

1. Cecchel, S. Materials and Technologies for Lightweighting of Structural Parts for Automotive Applications: A Review. *SAE Int. J. Mater. Manuf.* **2021**, *14*, 81–97. [CrossRef]
2. Birol, Y.; Ilgaz, O. Effect of cast and extruded stock on grain structure of EN AW 6082 alloy forgings. *Mater. Sci. Technol.* **2014**, *30*, 860–866. [CrossRef]
3. Anyalebechi, P.N. Effect of process route on the structure, tensile, and fatigue properties of aluminum alloy automotive steering knuckles. *Int. Foundry Res.* **2011**, *63*, 32–43.
4. Lee, K.; Kwon, Y.N.; Lee, S. Correlation of microstructure with mechanical properties and fracture toughness of A356 aluminum alloys fabricated by low-pressure-casting, rheo-casting, and casting–forging processes. *Eng. Fract. Mech.* **2008**, *75*, 4200–4216. [CrossRef]
5. Prucha, T. Metal Mold Processes—Gravity and Low Pressure Technology. In Proceedings of the American Foundry Society International Conference on Structural Aluminum Casting, Orlando, FL, USA, 2–4 November 2003.
6. Ou, J.; Wei, C.; Logue, S.; Cockcroft, S.; Maijer, D.; Zhang, Y.; Chen, Z.; Lateng, A. A study of an industrial counter pressure casting process for automotive parts. *J. Mater. Res. Technol.* **2021**, *15*, 7111–7124. [CrossRef]
7. Birol, Y.; Akdi, S. Cooling slope casting to produce EN AW 6082 forging stock for manufacture of suspension components. *Trans. Nonferrous Met. Soc. China* **2014**, *24*, 1674–1682. [CrossRef]
8. Atkinson, H.V. Semisolid processing of metallic materials. *Mater. Sci. Technol.* **2010**, *26*, 1401–1413. [CrossRef]
9. Midson, S.P.; Jackson, A. A Comparison of Thixocasting and Rheocasting. In Proceedings of the 67th World Foundry Congress, Harrogate, UK, 5–7 June 2006; Institute of Cast Metals Engineers (ICME): Tipton, UK, 2006; pp. 22/1–22/10, ISBN 9781604236767.
10. Kiuchi, M.; Kopp, R. Mushy/Semi-Solid Metal Forming Technology—Present and Future. *CIRP Ann.* **2002**, *51*, 653–670. [CrossRef]
11. The Aluminum Automotive Manual, Manufacturing—Casting Methods. Available online: https://european-aluminium.eu/wp-content/uploads/2022/11/aam-manufacturing-1-casting-methods.pdf (accessed on 21 May 2025).
12. Ghomashchi, M.R.; Vikhrovl, A. Squeeze casting: An Overview. *J. Mater. Process. Technol.* **2000**, *101*, 1–9. [CrossRef]
13. Zhang, M.; Zhang, W.-W.; Zhao, H.-D.; Zhang, D.-T.; Li, Y.-Y. Effect of pressure on microstructures and mechanical properties of Al-Cu-based alloy prepared by squeeze casting. *Trans. Nonferrous Met. Soc. China* **2007**, *17*, 496–501. [CrossRef]
14. Zhou, H.T.; Xu, S.X.; Li, W.D.; Wang, S.C.; Peng, Y. A study of automobile brake bracket formed by casting–forging integrated forming technology. *Mater. Des.* **2015**, *67*, 285–292. [CrossRef]
15. Möller, H.; Govender, G.; Stumpf, W.E.; Pistorius, P.C. Comparison of heat treatment response of semisolid metal processed alloys A356 and F357. *Int. J. Cast Met. Res.* **2010**, *23*, 37–43. [CrossRef]
16. Liu, X.; Wang, C.; Zhang, S.; Song, J.; Zhou, X.; Zha, M.; Wang, H. Fe-Bearing Phase Formation, Microstructure Evolution, and Mechanical Properties of Al-Mg-Si-Fe Alloy Fabricated by the Twin-Roll Casting Process. *J. Alloys Compd.* **2021**, *886*, 161202. [CrossRef]
17. Sigworth, G.K.; (Alcoa Primary Metals, Rockdale, TX, USA). Controlling Tensile Strength in Aluminum Castings. Private communication, 2006.
18. Cáceres, C.H.; Barresi, J. Selection of temper and Mg content to optimize the quality index of Al–7Si–Mg casting alloys. *Int. J. Cast Met. Res.* **2000**, *12*, 377–384. [CrossRef]
19. *ASTM E1251-24*; Standard Test Method for Analysis of Aluminum and Aluminum Alloys by Spark Atomic Emission Spectrometry. ASTM international: West Conshohocken, PA, USA, 2025.
20. Faccoli, M.; Dioni, D.; Cecchel, S.; Cornacchia, G.; Panvini, A. Optimization of heat treatment of gravity cast Sr-modified B356 aluminum alloy. *Trans. Nonferrous Met. Soc. China* **2017**, *27*, 1698–1706. [CrossRef]
21. Emadi, D.; Whiting, L.V.; Sahoo, M.; Sokolowski, J.H.; Burke, P.; Hart, M. Optimal heat treatment of A356.2 alloy. In Proceedings of the Light Metals, San Diego, CA, USA, 2–6 March 2003; pp. 983–989.
22. Dioni, D.; Cecchel, S.; Cornacchia, G.; Faccoli, M.; Panvini, A. Effects of artificial aging conditions on the mechanical properties of gravity cast B356 aluminum alloy. *Trans. Nonferrous Met. Soc. China* **2015**, *25*, 1035–1042. [CrossRef]
23. *ASTM E92-23*; Standard Test Methods for Vickers Hardness and Knoop Hardness of Metallic Materials. American Society for Testing and Materials: West Conshohocken, PA, USA, 2023.

24. *UNI EN ISO 6892–1*; Metallic Materials—Tensile Testing—Part 1: Method of Test at Room Temperature. ISO: Geneva, Switzerland, 2020.
25. Es-Said, O.S.; Lee, D.; Pfost, W.D.; Thompson, D.L.; Patterson, M.; Foyos, J.; Marloth, R. Alternative heat treatments for A357-T6 aluminum alloy. *Eng. Fail. Anal.* **2002**, *9*, 99–107. [CrossRef]
26. Callegari, B.; Lima, T.N.; Coelho, R.S. The Influence of Alloying Elements on the Microstructure and Properties of Al-Si-Based Casting Alloys: A Review. *Metals* **2023**, *13*, 1174. [CrossRef]